Instabilities of optical solitons and Hamiltonian singular solutions in a medium of finite extension

E. Assemat, Antonio Picozzi, Hans-Rudolf Jauslin, Dominique Sugny

Instabilities of optical solitons and Hamiltonian singular solutions in a medium of finite extension

E. Assémat, A. Picozzi, H. R. Jauslin, and D. Sugny*

Laboratoire Interdisciplinaire Carnot de Bourgogne (ICB), UMR 5209 CNRS-Université de Bourgogne, 9 Avenue A. Savary, Boîte Postale 47 870, F-21078 Dijon Cedex, France

(Received 3 May 2011; published 11 July 2011)

We analyze the role of soliton solutions and Hamiltonian singularities in the dynamics of counterpropagating waves in a medium of finite spatial extension. The soliton solution can become unstable due to the finite extension of the system. We show that the spatiotemporal dynamics then relaxes toward a Hamiltonian singular state of a nature different than that of the soliton state. This phenomenon can be explained through a geometrical analysis of the singularities of the stationary Hamiltonian system.

DOI: 10.1103/PhysRevA.84.013809 PACS number(s): 42.65.Tg, 05.45.−a, 02.30.Ik, 45.05.+x

I. INTRODUCTION

Nonlinear partial differential equations (PDE) which are completely integrable can be solved by means of the inverse scattering transform [1]. This method can be applied to a large variety of nonlinear equations, which have found applications in many different fields of physics and, in particular, in the context of nonlinear optics (see Ref. [2] for a recent overview). Among the solutions obtained by this approach, soliton solutions are known to play a key role because of their peculiar properties of stability.

The inverse scattering transform was originally developed for nonlinear systems of infinite extension, while the case of systems with finite spatial extension has only been addressed recently. The question of the stability of solitons in systems of finite length was recently analyzed by Kozlov and Wabnitz in Ref. [3]. Considering the example of a counterpropagating nonlinear wave interaction, they showed that the stationary soliton solution obtained in an infinitely extended medium becomes unstable when considered in a medium of finite extension. The soliton solutions of this system are the so-called polarization-domain wall solitons [4,5]. The model of Ref. [3] refers to the important practical situation in which two counterpropagating optical beams are injected in a continuous way from both ends of an optical fiber of length L. The numerical simulations reported in Ref. [3] reveal that even for a fiber length much larger than the characteristic width Δ of the soliton, the soliton solution exhibits an instability and relaxes, after a complex transient, toward a stationary state of a nature different than that of the initial soliton solution. Note that this type of relaxation process has also been the subject of several experimental studies in optical fibers and is now called "polarization attraction" [4,6,7], due to its role in the dynamics of polarizations of the optical beams.

From a different perspective, we recently showed that the stationary states selected by the spatiotemporal dynamics can be associated with *Hamiltonian singular solutions* of the stationary system. These stationary solutions belong to a two-dimensional object of the associated phase space, the so-called *singular torus*, which plays the role of an attractor for the nonlinear system [8,9]. The natural important problem is to analyze the relation between the stability properties of the soliton solution and the structure of the singular Hamiltonian solutions of the corresponding stationary system.

In this paper, we consider two models of the same general class. One of them has a single isolated singular torus, while the other one, analyzed in Ref. [3], is shown to have a one-parameter family of singular tori. We first show that the soliton solution belongs to the ensemble of singular Hamiltonian solutions of the associated stationary system. *The analysis reveals that when the singular torus of the Hamiltonian system is isolated then the space-time dynamics is asymptotically attracted toward the soliton solution, which is thus stable. Conversely, the soliton becomes unstable in the presence of a continuous family of Hamiltonian singular tori and the dynamics relaxes toward another stationary state of this family.* These examples indicate that the geometrical analysis of the singularities of the stationary Hamiltonian system appears to be the appropriate theoretical framework to study nonlinear wave systems in a medium of finite spatial extension. In particular, the fact that the selected stationary states can strongly differ from the soliton solution can be explained through the analysis of the topological properties of the corresponding singular tori.

Besides its fundamental interest, the process of polarization attraction discussed here has applications as a polarizer performing polarization of light with almost 100% efficiency, in contrast with standard polarizers that unavoidably waste 50% of unpolarized light (also see Ref. [10]). This aspect is presently attracting great interest because of the possibility of achieving a repolarization of optical transmission lines in telecommunication systems [7,11].

We consider the one-dimensional counterpropagating configuration of the four-wave interaction. Different models describing a variety of situations have been introduced in the literature. Using the Stokes formalism, the equations governing the polarization dynamics of the counterpropagating beams can be written in the following general form:

$$\begin{aligned} \frac{\partial \vec{S}}{\partial t} + \frac{\partial \vec{S}}{\partial z} &= \vec{S} \times (\mathcal{I}\vec{J}) + \mathcal{F}_S(\vec{S},\vec{J}), \\ \frac{\partial \vec{J}}{\partial t} - \frac{\partial \vec{J}}{\partial z} &= \vec{J} \times (\mathcal{I}\vec{S}) + \mathcal{F}_J(\vec{S},\vec{J}). \end{aligned} \tag{1}$$

The Stokes vectors $\vec{S} = (S_x, S_y, S_z)$ and $\vec{J} = (J_x, J_y, J_z)$ describe, respectively, the polarization states of the forward

*dominique.sugny@u-bourgogne.fr

and backward beams on the Poincaré sphere. The matrix $\mathcal{I}$ is diagonal and '$\times$' denotes the vector product, while the functions $\mathcal{F}_S$ and $\mathcal{F}_J$ are polynomials of the Stokes vectors $(\vec{S},\vec{J})$, which account for the nonlinear self-interaction terms of the waves. The radii of the forward and backward spheres, S_0 and J_0, are related to the signal and pump powers. We normalized the variables with respect to the nonlinear interaction time $\tau_0 = 1/(\gamma S_0)$ and length $\Lambda_0 = v\tau_0$, where γ is the nonlinear coefficient and v the group velocity of the waves. The variables can be recovered in standard units through $t \to t\tau_0, z \to z\Lambda_0$, and $(\vec{S},\vec{J}) \to (\vec{S},\vec{J})S_0$. In the limit where the two functions $\mathcal{F}_{S,J}(\vec{S},\vec{J})$ vanish, the PDE system (1) is integrable in an infinite medium [2,12].

II. MODEL I

We consider here the example of Ref. [3] defined by $\mathcal{I} = \mathrm{diag}(1,-1,-2)$, which is denoted system I in the following. The choice of this particular example stems from the fact that it is known to model light propagation in a birefringent spun fiber [13]. The corresponding soliton solution is a zero-velocity domain wall [5]:

$$\begin{aligned} S_x^s &= -\tanh(\sqrt{2}z), \quad J_x^s = -\tanh(\sqrt{2}z), \\ S_y^s &= -\frac{1}{\sqrt{3}}\mathrm{sech}(\sqrt{2}z), \quad J_y^s = -\frac{1}{\sqrt{3}}\mathrm{sech}(\sqrt{2}z), \\ S_z^s &= \frac{\sqrt{6}}{3}\mathrm{sech}(\sqrt{2}z), \quad J_z^s = -\frac{\sqrt{6}}{3}\mathrm{sech}(\sqrt{2}z). \end{aligned} \tag{2}$$

The solution (2) is a stationary solution of Eq. (1). Moving soliton solutions can also exist for different powers of the beams ($S_0 \neq J_0$), but they are not relevant to the finitely extended medium discussed here. In the following we assume $S_0 = J_0$. The first step of our analysis consists of studying the singularities of the stationary system associated with system (1) [8]. It is straightforward to see that this system is an ordinary differential equation (ODE) with the Hamiltonian

$$H = -S_x J_x + S_y J_y + 2S_z J_z, \tag{3}$$

where the Poisson brackets are defined by $\{S_i,S_j\} = \varepsilon_{ijk}S_k$, $\{J_i,J_j\} = -\varepsilon_{ijk}J_k$, ε_{ijk} being the completely antisymmetric tensor. This ODE system is integrable since it admits an additional constant of the motion $K = S_z + J_z$. We construct the energy-momentum diagram (H,K), which indicates the location of the singularities in the set of the possible values of H and K. More precisely, the Liouville-Arnold theorem [14] shows that the phase space is foliated by invariant sets, labeled by the values H and K. In general, the invariant sets are standard tori, but there are points of this diagram for which the corresponding tori are singular [15]. The singular sets of this diagram correspond to the points where the two gradients ∇H and ∇K are collinear (we refer the reader to Refs. [8,9,16] for an explicit construction of a similar diagram). In the present model, the energy-momentum diagram contains a continuous line of singularities whose corresponding set in the original phase space is a bitorus, i.e., a singular torus consisting of two tori glued along a circle [see Fig. 1(a)] [15]. A bitorus can also be viewed as the Cartesian product of an eight figure with a circle. The soliton solution (2) is a particular case of a Hamiltonian singular solution that belongs to the torus located

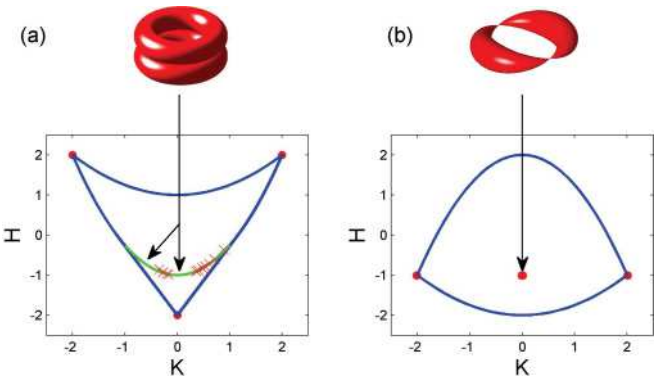

FIG. 1. (Color online) Energy-momentum diagram of stationary model I (a) and of model II (b). The green (light gray) curve in panel (a) denotes the singular line of bitori. The *unstable* soliton solution (2) is a particular point of the singular line located at $(H=-1,K=0)$. The crosses on the singular line locate the positions of the stationary states obtained by solving numerically the PDE model I for different fiber lengths L (from $L=3$ to $L=10$). The energy-momentum diagram for model II (b) has an isolated singularity located at $(K=0,H=-1)$, which corresponds to a doubly pinched torus. This singularity coincides with the position of the soliton solution (5). In this case, the PDE space-time dynamics relaxes to the *stable* soliton state.

at $(K=0,\ H=-1)$ in the energy-momentum diagram. The trajectory of the soliton solution (2) is schematically illustrated on the corresponding bitorus in Fig. 2(a) [red (thick gray) line]. Note that the trajectory starts and ends on the singular circle of the bitorus.

We perform numerical simulations of the space-time system I. We start the simulation from the soliton solution (2) truncated in the finite interval $[0,L]$, as well as from a homogeneous solution (see the dashed lines in Fig. 3). The boundary conditions at both ends of the optical fiber are kept fixed to the corresponding values of the initial wave, i.e., $\vec{S}(z=0,t) = \vec{S}(z=0,t=0)$, $\vec{J}(z=L,t) = \vec{J}(z=L,t=0)$. In the case of the homogeneous initial condition, the boundary conditions are the same as those for the soliton initial condition, $\vec{S}(z=0,t) = \vec{S}^s(z=0)$, $\vec{J}(z=L,t) = \vec{J}^s(z=L)$. For these two sets of initial conditions, the simulations reveal that, after a complex transient, the system relaxes toward the *same stationary state*. As illustrated by the continuous lines in Fig. 3, this stationary state is completely different from the soliton solution (2), which confirms the previous results of Ref. [3] where the instability of the soliton in a finitely extended system is reported.

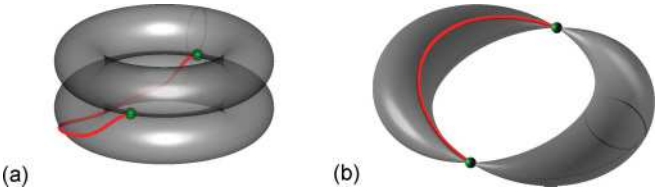

FIG. 2. (Color online) Trajectories of the soliton solutions on the bitorus for model I (a) and on the doubly pinched torus for model II (b).

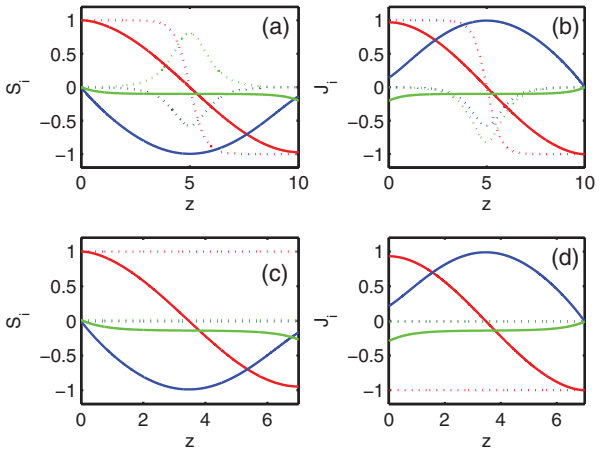

FIG. 3. (Color online) Numerical integration of the PDE model I showing the instability of the soliton solution: (a, b) Soliton solution (2) considered as the initial condition (dashed lines) and corresponding stationary state asymptotically selected by the space-time dynamics (continuous lines). Panel (a) displays the $\vec{S}$ components, and panel (b) displays the $\vec{J}$ components. The x, y, and z components are represented in red (dark gray), blue (black), and green (light gray), respectively. (c, d) Same as in panels (a) and (b), but starting from a homogeneous solution (see the text): the system relaxes toward the same singular stationary state as in panels (a) and (b).

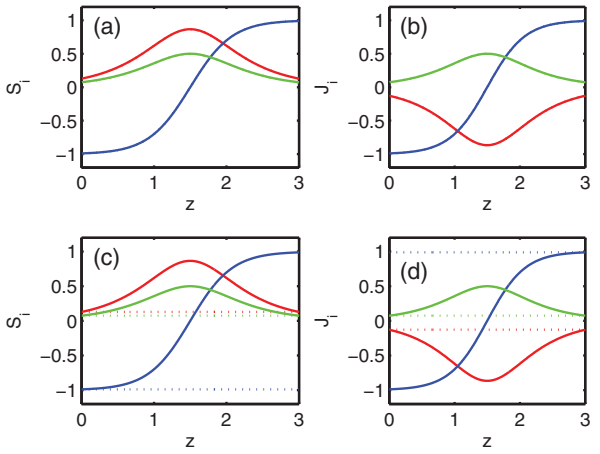

FIG. 4. (Color online) Same as Fig. 3 but for model II Eq. (4): the numerical simulations show that the soliton solution (5) is stable.

The simulations show that the stationary state selected by the spatiotemporal dynamics always lies in the neighborhood of the line of singular bitori, as illustrated by the crosses in Fig. 1(a). The stationary state is shown to converge exponentially toward the line of singular tori as $L \to +\infty$. However, this convergence occurs for values of K that differ substantially from $K = 0$, i.e., far from the bitorus of the soliton solution [see Fig. 1(a)]. These results show that, in order to understand the long time behavior of the PDE system, it is not sufficient to consider the soliton solution, but one has to take into account the more general singular Hamiltonian solutions.

III. MODEL II

We now consider the PDE model that describes some of the experiments of polarization attraction reported in Refs. [4,6,7]:

$$\begin{aligned} \frac{\partial \vec{S}}{\partial t} + \frac{\partial \vec{S}}{\partial z} &= \vec{S} \times (\mathcal{I}\vec{S}) + 2\vec{S} \times (\mathcal{I}\vec{J}), \\ \frac{\partial \vec{J}}{\partial t} - \frac{\partial \vec{J}}{\partial z} &= \vec{J} \times (\mathcal{I}\vec{J}) + 2\vec{J} \times (\mathcal{I}\vec{S}), \end{aligned} \tag{4}$$

where the diagonal matrix reads $\mathcal{I} = \mathrm{diag}(-1,0,-1)$. This system is termed model II.

The geometrical analysis of the stationary ODE system (4) has been reported in Refs. [8,9]. Here we study the relation between this geometrical approach and the soliton solutions. Note that the term "soliton" is used here in its loose sense, since the PDEs (4) are not integrable (self-interaction terms are considered) and thus only admit solitary-wave solutions. The stationary (t-independent) system (4) is an integrable ODE with the Hamiltonian

$$H = 2(S_x J_x + S_z J_z) - \tfrac{1}{2}\left(S_y^2 + J_y^2\right),$$

which Poisson commutes with the constant of motion $K = S_y - J_y$. The corresponding energy-momentum diagram is reported in Fig. 1(b). In contrast to model I, the diagram is now characterized by an isolated singularity associated with a doubly pinched torus located at $K = 0$ and $H = -1$. The stationary system (4) admits a soliton solution of the form

$$\begin{aligned} S_x^s &= \frac{\sqrt{3}}{2}\mathrm{sech}(\sqrt{3}z), \quad J_x^s = -\frac{\sqrt{3}}{2}\mathrm{sech}(\sqrt{3}z), \\ S_y^s &= \tanh(\sqrt{3}z), \quad J_y^s = \tanh(\sqrt{3}z), \\ S_z^s &= \frac{1}{2}\mathrm{sech}(\sqrt{3}z), \quad J_z^s = \frac{1}{2}\mathrm{sech}(\sqrt{3}z). \end{aligned} \tag{5}$$

As shown in Fig. 1(b), the position of this soliton solution coincides with the position of the pinched torus ($K = 0$, $H = -1$). The soliton trajectory on the singular torus starts and ends at the two pinch points. The solution (5) has the same structure as the soliton solution of the integrable system I. However, the spatiotemporal dynamics has a different behavior. Indeed, we perform the same type of space-time numerical simulations reported in Fig. 3 but with the PDE model II (4). The simulations now reveal that the soliton is stable and plays the role of an attractor for the finitely extended spatiotemporal dynamics. This is illustrated in Fig. 4, which shows that the dynamics asymptotically converges toward the stable soliton solution (5).

IV. DISCUSSION

The different behaviors observed for systems I and II can thus be explained by the structure of the energy-momentum diagrams. In both models I and II the dynamics is characterized by a relaxation toward a stationary state that lies in the neighborhood of a singular torus. However, in contrast with model II where the unique isolated singular torus coincides with the soliton solution (5), in model I there exists a continuous family of Hamiltonian singular solutions which differ from the soliton solution (2). Despite the apparent similarity of

the two soliton solutions, i.e., a pair of sech-shaped functions for the x and z components, and a tanh function for the y component, a completely different spatiotemporal dynamics is observed. These results indicate that the stability of a soliton solution in a finitely extended medium can be understood from the nature and the distribution of singular tori in the energy-momentum diagram.

Note that although the PDEs that model the experiments are not PDE integrable (in an infinite medium), the relaxation toward a stationary state is of the same nature as that discussed in the PDE integrable model I. In particular, we have checked that the self-interaction terms of model II that break the integrability do not change qualitatively either the energy-momentum diagram (which still presents an isolated doubly pinched torus) or the spatiotemporal dynamics. Based on these numerical simulations, we conjecture that the PDE integrability of these systems does not play any role in the relaxation phenomenon and in the stability of the soliton solution. Conversely, this instability can be explained through the geometrical analysis of the singularities of the ODE integrable stationary Hamiltonian system, which thus appears as the appropriate theoretical framework to study nonlinear physical systems of finite spatial extension. The mathematical analysis of the different properties presented in this paper is a forthcoming goal. As a first step, following the recent results of Ref. [17], one can consider the stability of the soliton solution of the wave propagation in a periodic grating. Indeed, given the generality of the mathematical treatment [8,15], the analysis developed here is expected to be transposable to different kinds of Hamiltonian physical systems of finite spatial extension. In this framework, another example is given by the degenerate configuration of the resonant three-wave interaction [18] which also presents a one-parameter family of singular tori. However, these tori are curled and of a different nature than the line of bitori of this paper [16]. An open question is then to study the problem of the stability of the soliton solutions in this type of nonlinear system.

[1] D. L. Faddeev, L. Takhtajan, and A. G. Reyman, *Hamiltonian Methods in the Theory of Solitons* (Springer, New York, 2007); G. L. Lamb, *Elements of Soliton Theory* (Wiley & Sons, New York, 1980); M. A. Ablowitz and P. A. Clarkson, *Solitons, Nonlinear Evolution Equations and Inverse Scattering* (Cambridge University Press, Cambridge, UK, 1992).

[2] A. Degasperis, J. Phys. A **43**, 434001 (2010).

[3] V. V. Kozlov and S. Wabnitz, Lett. Math. Phys. **96**, 405 (2011).

[4] S. Pitois, G. Millot, and S. Wabnitz, Phys.Rev. Lett. **81**, 1409 (1998); J. Opt. Soc. Am. B **18**, 432 (2001).

[5] M. V. Tratnik and J. E. Sipe, Phys. Rev. Lett. **58**, 1104 (1987); D. David, D. D. Holm, and M. V. Tratnik, Phys. Rep. **187**, 281 (1990); S. Wabnitz, Opt. Lett. **34**, 908 (2009); IEEE Photonics Technol. Lett. **21**, 875 (2009).

[6] S. Pitois, A. Picozzi, G. Millot, H. R. Jauslin, and M. Haelterman, Europhys. Lett. **70**, 88 (2005).

[7] S. Pitois, J. Fatome, and G. Millot, Opt. Express **16**, 6646 (2008); J. Fatome, S. Pitois, P. Morin, and G. Millot, *ibid.* **18**, 15311 (2010).

[8] D. Sugny, A. Picozzi, S. Lagrange, and H. R. Jauslin, Phys. Rev. Lett. **103**, 034102 (2009).

[9] S. Lagrange, D. Sugny, A. Picozzi, and H. R. Jauslin, Phys. Rev. E **81**, 016202 (2010); E. Assémat, A. Picozzi, H. R. Jauslin, and D. Sugny, Opt. Lett. **35**, 2025 (2010).

[10] E. Heebner, R. S. Bennink, R. W. Boyd, and R. A. Fisher, Opt. Lett. **25**, 257 (2000); A. Picozzi, Opt. Express **16**, 17171 (2008).

[11] V. V. Kozlov, J. Nuno, and S. Wabnitz, J. Opt. Soc. Am. B **28**, 100 (2011).

[12] V. E. Zakharov and A. V. Mikhailov, JETP Lett. **45**, 349 (1987); I. V. Cherednik, Sov. J. Nucl. Phys. **33**, 144 (1981).

[13] V. V. Kozlov and S. Wabnitz, Opt. Lett. **35**, 3949 (2010).

[14] V. I. Arnold, *Mathematical Methods of Classical Mechanics* (Springer-Verlag, New York, 1989).

[15] K. Efstathiou and D. A. Sadovskií, Rev. Mod. Phys. **82**, 2099 (2010); R. H. Cushman and L. M. Bates, *Global Aspects of Classical Integrable Systems* (Birkhäuser, New York, 1997); D. Sugny, P. Mardesic, M. Pelletier, A. Jebrane, and H. R. Jauslin, J. Math. Phys. **49**, 042701 (2008); K. Efstathiou and D. Sugny, J. Phys. A **43**, 085216 (2010).

[16] E. Assémat, C. Michel, A. Picozzi, H. R. Jauslin, and D. Sugny, Phys. Rev. Lett. **106**, 014101 (2011).

[17] M. Grenier, H. R. Jauslin, C. Klein, and V. Matveev (unpublished).

[18] D. J. Kaup, A. Reiman, and A. Bers, Rev. Mod. Phys. **51**, 275 (1979).